ION BOMBARDMENT INDUCED DIFFUSION: A CASE STUDY ON A SPUTTERED Ag/Ni LAYERED SYSTEM**

D. MARTON* and J. FINE

Surface Science Division
National Institute of Standards and Technology
Gaithersburg, MD 20899, USA
Received, June 27, 1989

Introduction

The layered Ag/Ni system has been shown to exhibit surface segregation of Ag when Ag layer buried between two Ni layers is sputter profiled at room temperature (J. Fine et al., 1983). While that study was concerned with the analysis of radiation induced segregation (RIS), it also demonstrated the role of bombardment enhanced diffusion in the transport of Ag atoms to the surface. The segregation rate was shown to obey first order kinetic equations, and segregation rates for 1 keV and 4 keV sputtering were determined.

This type of RIS is currently of interest in surface analysis as a possible source of significant depth profile distortion due to ion bombardment. RIS involves composition redistributions either via collisional (or ballistic) mixing and spikes, or via radiation enhanced diffusion (RED). These two classes of phenomena differ both in the ranges and in the times involved in each: mixing and the associated spikes extend, according to binary collision calculations (F. Davarya et al., 1983) to 2—4 nm at 1—4 keV Ar^+ ion bombardment and dissipate in a matter of 10^{-10} s or less. RED is, however, a long range and long time process. This difference between the cascade mixing and RED was probably first recognized by Chu et al. (W. K. Chu et al., 1976), who observed a "mixing depth" in Al-Cu alloys of about 30 nm under keV Xe bombardment; the depth of mixing attributable to cascade mixing alone would have been certainly less than 10 nm. Ho (P. S. Ho, 1978) developed a diffusion model to describe the observations of Chu et al., and this model, with some modification is still in use. Ho's model cannot be applied, however, directly to immiscible systems, because it presumes the existence of a homogeneous mix prior to ion impact.

Experimental studies of radiation enhanced diffusion (RED) usually consist of 3 steps (R. R. Hart et al., 1975, J. E. Hobbs et al., 1981 and 1985, D. G. Swartzfager et al., 1981, L. Kornbilt et al., 1985, W. Vandervorst et al.,

* On leave from the Technical University Budapest, Hungary
** Dedicated to Prof. J. Giber on the ocassion of his 60th birthday.

1986, D. Farkas et al., 1986, R. Collins, 1985): (1) a specimen is prepared containing a marker of known depth distribution; (2) the specimen is then irradiated (ion bombarded) and (3) a depth profile of the marker is obtained (this last step often includes the observation of RIS). Studies of bombardment induced RED are often complicated due to erosion of the sample during irradiation (R. Collins, 1985). The depth profiles obtained in step 3 often are also obtained by sputter profiling (usually at an energy much lower than that used in step 2) which also can lead to additional complexity in evaluation.

The aim of this present work has been the analysis of RED occuring during constant ion bombardment conditions (thus combining steps 2 and 3) using Auger depth profiling techniques. For this, multilayered Ag/Ni samples were sputter-depth profiled and the shape of the depth profiles of the Ag layers obtained under steady-state conditions were described using a simple model, which included mainly roughening and RED, the latter being characterized with an effective diffusion rate. This approach has the advantage that the results obtained are directly applicable to Auger (and SIMS) depth profiling; the results of such an analysis should allow us to differentiate those separate contributions due to both roughening of the surface and RED. Our evaluation of the Ni and Ag Auger depth profiles was based on being able to separate these two contributions. This separation could be then confirmed by an independent measurement of surface roughness using off-specular light scattering techniques, since the light scattering is directly related to surface roughness. We have carried out in-situ surface roughness measurements on the same samples and on the same surfaces we studied by AES depth profiling. Our light scattering results strongly support those results described in the present paper, but further details will be published elsewhere (D. Marton and J. Fine, in print).

The temperature dependence of the diffusion rate of ion bombardment induced RED of Ag in Ni was also investigated. Previous temperature-dependent measurements of the RED rate (D. G. Swartzfager et al., 1981, Li et al., 1985, Lam et al., 1985 and 1988, Hoff et al., 1988) indicate that this rate increases with temperature; this increase is qualitatively consistent with an increase in atom mobility under steady-state defect concentration (even though the activation energy for RED is much less than the migration energy). We have found, however, specifically for the case for Ag diffusion in Ni, new evidence that suggests that at elevated temperatures it is possible to anneal those defects responsible for diffusion, and so to virtually eliminate the RED of Ag (D. Marton et al., PRL, 1988). These results provide new insight into RED transport processes, show that atom mobility (i.e., the migration energy) is not the only factor contributing to the temperature dependence, and demonstrate that in certain material systems annealing effects tend to dominate this dependence.

2. Experiments and results

Both RED and surface roughening which result from ion bombardment of the Ag/Ni system were analysed using multilayered Ag/Ni thin film structures. These structures consist of five thin (3—4 nm) Ag layers alternately deposited between six thick (50 nm) Ni layers. Such samples were produced by sputter deposition using polished Si substrates that had been coated, in situ, with amorphous Si prior to the deposition of the metal films and are similar to those previously described (J. Fine et al., 1983). Stylus measurements indicated that the r.m.s. surface roughness of the samples prior to sputtering was less than 1 nm.

Sputter-depth profiling of these Ag/Ni samples was carried out using Ar^+ ions of both 1 keV and 4 keV energy. A differentially pumped ion gun produced a fine focussed beam that was scanned over about 2×2 mm^2 at total beam currents in the 50 to 500 nA range; Auger analysis was performed using a high resolution single-pass cylindrical mirror analyzer described earlier (J. Fine et al., 1985). The base pressure in the vacuum system during the experiments described here was typically 3×10^{-9} Torr. Auger-electron spectra excited by a primary electron beam of 2500 eV energy (50—200 nA) were recorded in a EN(E) mode; digital background subtraction techniques were employed to obtain high precision depth profiles. The elements detected were Ni (LMM line, 844 eV), Ag (MNN line, 349 eV) and nitrogen (KLL line, 375 eV).

The Ag/Ni specimens were mounted on a sample holder containing an electrical heater and a chromel-alumel thermocouple. During the Auger depth profiling the temperature could be varied from 299 to about 800 K. The stability and the accuracy of the temperature readings were estimated to be better than ± 1 K for relatively low temperatures (up to 350 K) and not worse than ± 5 K at the high temperature limit.

2.1. The range of damage and the time scale

In a series of measurements, the top Ni layer of the Ag/Ni specimens was sputtered for various times and the sputtering was stopped before the Ag Auger signal rose above the background level (approximately 1at%). An example of such an experiment is shown in Fig. 1. In this case, sputtering was stopped at $t_1 = 51.7$ min and resumed at $t_2 = 67$ min; the Ag peak was detected at $t = 83.4$ min. From these data, and the known layer thicknesses, and making simple assumptions for the sputtering rates, the distance between the Ni surface at t_2 and the Ag layer can be obtained. Segregation occurs, however, only when the sputtered surface at t_2 is closer to the Ag layer than some minimum

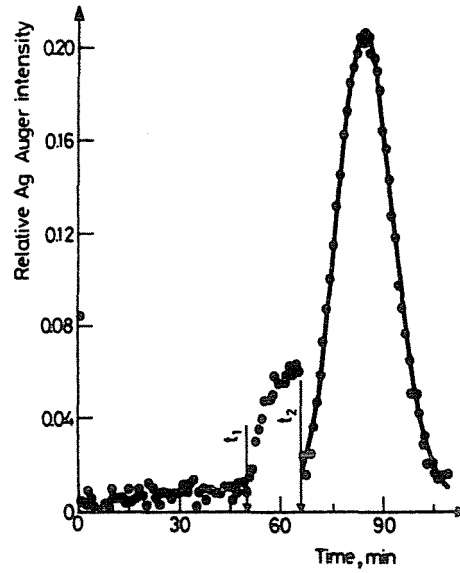

Fig. 1. Auger depth profile of an Ag layer ($E_p = 1$ keV). The ordinate is the relative $N(E)$ yield for Ag. The measured Ag data are shown as *, the solid line through the Ag data represents a fit corresponding to eq. (5). The depth profiling was stopped at t_1. Segregation of Ag was observed from t_1 to t_2, when sputtering was resumed

migration distance. In a series of such experiments, the largest such distance between the sputtered surface and the Ag layer can be determined. This distance is the experimental Ag range attributable to ion impact in our experiments, denoted by z_0. Our experiments show that $z_0 = 15.3 \pm 5$ nm for 1 keV and 18.5 ± 0.5 nm for 4 keV Ar^+ sputtering, respectively.

As it is evident from Fig. 1, but was shown in much more detail earlier (J. Fine et al., 1983), the time scale of the Ag RIS process is of the order of minutes. Thus it is clear, from both the range and time data, that the transport process leading to the surface segregation of the Ag atoms in this case, is diffusion rather than ion mixing.

2.2. RED experiments at room temperature

A typical AES sputter depth profile is shown in Fig. 2a. The abscissa is the sputtering time, which can be readily transformed to a depth scale using known layer thicknesses. The evaluation procedure for each Ni and Ag depth profile, shown in Fig. 2a, is based on a series of assumptions and simplifications.

Each depth profile of a given individual Ag layer is analysed independently. Each such depth profile resembles a Gaussian in shape but is asymmetric,

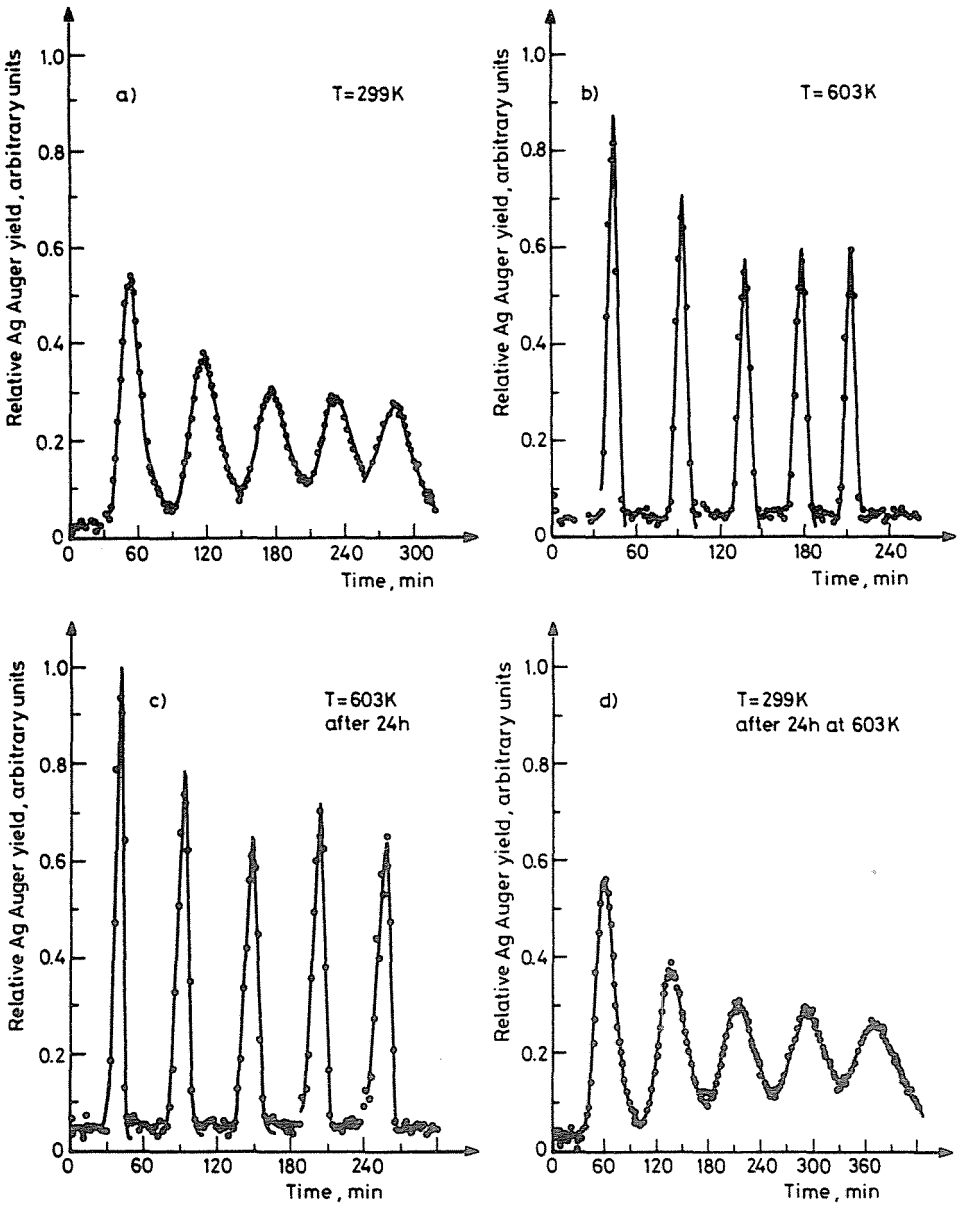

Fig. 2. A sequence of Auger-electron spectroscopy depth profiles obtained with 4 keV Ar^+ sputtering. a) −299 K, b) −603 K, c) −603 K after 24 h, and d) −299 K after the heating cycle. The measured points are *, the fitted curves are the solid lines, computed according to eq. (5)

having a steeper slope at earlier sputtering times. We propose that each of these Ag profiles is the result of the superposition of a Gaussian (symmetric) and a RED (asymmetric) profile. The width of the Gaussian profile is determined mainly by surface roughness, although a small contribution from other factors is not excluded. One such factor is the thickness of the Ag layer, another is the escape depth of Auger electrons, a third is interface broadening due to cascade mixing, and a fourth is that due to thermal diffusion. Since these factors are small and since there is no evidence to suggest that the surface roughness distribution is anything other than normal, our assumption is that all these combined factors yield a Gaussian depth profile shape:

$$c=(2^{1/2}c_0/\Delta z_R)\exp[-2(z-z_0)^2/\Delta z_R^2], \tag{1}$$

where c_0 depends on the total number of the Ag atoms per surface area in a single silver layer, z is the depth coordinate, directed perpendicular to the surface, and Δz_R^2, can be expressed as

$$\Delta z_R^2=\Delta z_r^2+d_{Ag}^2+l_e^2+\Delta z_c^2+\Delta z_d^2, \tag{2}$$

in which Δz_r, Δz_c and Δz_d are the contributions of surface roughness, cascade mixing, and thermal diffusion respectively, and l_e is the inelastic mean free path of Auger electrons. The thickness of the Ag layer is given by d_{Ag}.

Furthermore, we assume that RED starts when the sputtered surface is at a distance of z_0 from the Ag layer, and that it continues at a constant rate after that. This will lead, according to standard diffusion theory for a planar source of negligible thickness at z_0, to a concentration profile described by the equation (e.g. P. G. Shewmon, 1963):

$$c=c_0(4Dt)^{-1/2}\exp[-(z-z_0)^2/4Dt], \tag{3}$$

where D is the (effective) diffusion coefficient and t is the diffusion time. Time t is related to depth z, and the sputtering rate S, according to the above definition for z_0 by

$$z=St. \tag{4}$$

Note that time t for each Ag layer is measured separately.

Combining equations (1)—(4) we obtain an equation which describes the measured depth profiles:

$$c=c_0(4Dt+\Delta z_R^2/2)^{-1/2} * \exp/-(St-z_0)^2(4Dt+\Delta z_R^2/2)^{-1}]. \tag{5}$$

Depth profiles, containing c vs t information, are used in a computer fitting program to calculate c_0, D and Δz_R, as well as a background for c. This equation can be used to obtain very precise fits to the asymmetric Ag-layer sputter depth profiles (D. Marton et al., 1988).

The model described above allows us to calculate interface broadening values for each sputtered Ag layer. In this procedure we first calculate the maximal Ag concentration. Then the sputtering rate, S is evaluated, assuming that the sputtering yield of the Ag-Ni mix is the weighted average of the elemental sputtering yields of Ag and Ni. The variation of S within the Ag layers was neglected owing to the small variation of the Ag concentration in the Ag depth profiles. Now, eq. (5) is used to fit the experimental depth profile and c_0, D and Δz_R are determined from the fit.

The interface broadening due to the surface roughness, Δz_r is then obtained from eq. (5). Here $l_e = 0.8$ nm (Ag at 375 eV, J. C. Ashley et al., 1982) has been used for all measurements. Values of Δz_c for various sputtering ions and energies are available from calculations based on Monte-Carlo methods (F. Davarya et al., 1983). The values used here are 2 nm for $E_p = 1$ keV and 4 nm for $E_p = 4$ keV bombardment. Thermal interdiffusion in the Ag/Ni system is probably very small due to the low solubility of silver in nickel (M. Hansen, 1958). The thermal diffusion contribution was also checked by carrying out some experiments at elevated temperatures. After a heat treatment of the sample in vacuum at 330°C for 24h no change in the depth profiles could be detected (cf. Fig. 2a—d). Thus Δz_d is neglected in the present calculations.

The total interface width obtained in our measurements is in part due to RED. This part can be characterized by the quantity

$$\Delta z_D = (8Dz_0/S)^{1/2}, \tag{6}$$

the "diffusion interface width" which plays an analogous role to Δz_R in eq. (5) for $t = z_0/S$. In our experiments we found that both the total interface broadening $\Delta z = (\Delta z_D^2)^{1/2}$ and Δz_r increase with the energy of the bombarding ions and with the depth (D. Marton et al., 1988). The analysis of the data clearly shows also that Δz_D is independent of the depth, and thus the depth dependence of the interface width is due to the roughening of the surface. This could be expected since there is no reason why the RED process would be affected by the depth, whereas the roughening of the surface is expected to increase as the square root of the depth (D. Marton and J. Fine, 1987).

2.3. The effect of current density

Diffusion coefficients obtained from experimental depth profiles of Ag, using eq. (5) to fit the data, are plotted in Fig. 3 as a function of sputtering rates S_{Ni}. Results obtained with both 1 keV and 4 keV sputtering energies, E_p, are described by linear equations:

$$D = 1.22 \times 10^{-17} + 1.75 \times 10^{-15} S_{Ni}$$

$$(r = 0.9710, \quad n = 43, \quad E_p = 1 \text{ keV}) \tag{7a}$$

and

$$D = 1.35 \times 10^{-17} + 9.05 \times 10^{-15} S_{Ni}$$
$$(r = 0.9764, \quad n = 29, \quad E_p = 4\,\text{keV}) \tag{7b}$$

where D is in units of cm^2/s and S_{Ni} is in nm/s; r is the regression coefficient and n is the number of data points taken into consideration.

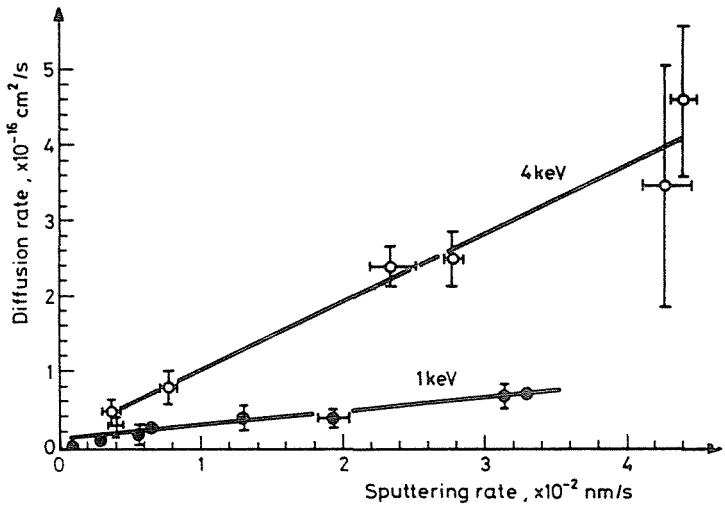

Fig. 3. RED rates obtained from AES depth profiling experiments vs. sputtering rate. Each point corresponds to one set of multilayer profile measurements, i.e. several (in most cases 5) data points. The error bars correspond to the standard deviation of these points. ○ — 1 keV, × — 4 keV energy of incident ions

In Fig. 3, data obtained in the same sputtering profile (constant sputtering rate) from a number of Ag layers at different depths are shown as a single point, with an error bar corresponding to the scatter of the sputtering rate and diffusion rate of the various layers. The diffusion rates are plotted against the sputtering rates rather than against current densities, as the latter are not easily measurable. Since the sputtering rates are proportional to the current densities for a given bombarding ion energy, equations (7a, b) describe linear dependences of the measured diffusion rates on the ion beam current density. The $D(0)$ values (which correspond to a linear extrapolation of S_{Ni} to zero, about 1.3×10^{-17} cm^2/s) are probably due to measurement uncertainties. Nevertheless, it is quite clear that the RED rates are proportional to the sputtering rates, which themselves are proportional to the current densities at any given energy of the Ar^+ ions.

2.4. Temperature dependence of RED

The first results discussed here address the question of whether there are any irreversible effects introduced by moderate annealing of the Ag/Ni samples. Initially the sample was sputter depth profiled at room temperature (cf. Fig. 2a). Then, on the same sample and under the same sputtering conditions, depth profiles were obtained at 603 K as shown in Figs 2b and 2c. The measurement shown in Fig. 2b was initiated immediately after the sample had reached this temperature; the measurement in Fig. 2c is a depth profile obtained after the sample was held at this same temperature for 24 h. One day later a fourth depth profile was again recorded at room temperature (Fig. 2d). There appear to be no significant differences between the two depth profiles obtained at the same temperature, whether at 299 or 603 K. The profiles obtained at different temperatures, however, do differ significantly: the depth profiles at 603 K are better resolved and do not exhibit the asymmetry characteristic of the room temperature data. This lack of irreversible effects allows us to conclude that at temperatures up to 603 K, no additional structural or compositional changes occur. Also, apparently no measurable diffusion takes place at 603 K (or at 299 K) until the sputtering process is begun. The lack of a symmetry coupled with the decrease in width of the depth profiles obtained at elevated temperatures demonstrates that a dramatic decrease of the diffusion rate takes place when the sputtering temperature is raised from 299 to 603 K.

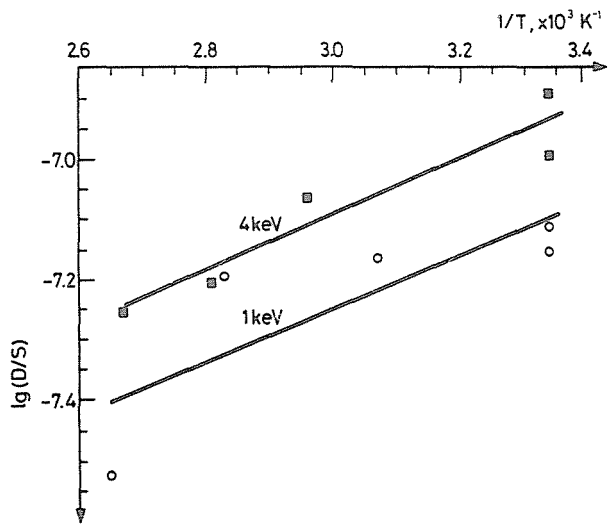

Fig. 4. Arrhenius plots of the ratio of the RED rate to the sputtering rate. ○ — 1 keV and □ — 4 keV data. Each point corresponds to the average rate obtained from all of the 5 Ag layers measured in each profile

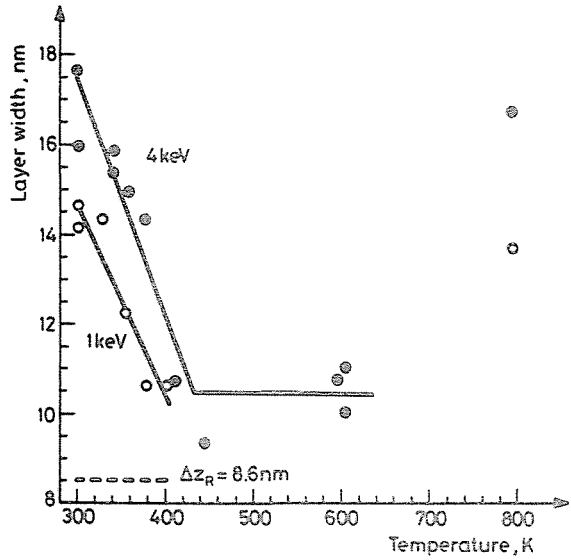

Fig. 5. The temperature dependence of the total layer width (Δz); for 1 keV (○) and 4 keV (□) ion bombardment. The average value of the symmetric layer width for the temperatures 299—404 K ($\Delta z_R = 8.6 \pm 1.1$ nm) is shown as a dashed line. All data in this figure were obtained on the first Ag layer (depth 50 nm). The solid lines are drawn to guide the eye

The temperature dependence of the diffusion rate determined with eq. (5) is shown in Fig. 4 in the form of Arrhenius plots of the diffusion rates divided by the sputtering rate, S, used in each measurement. The use of D/S instead of D is necessary because D is linearly dependent on S. The "activation energies" determined for the 1- and 4-keV data are $Q_1 = -0.038$ and $Q_4 = -0.040$ eV, respectively (these slopes are significant on the 10% and 2.5% level, respectively). The difference between these two values is well within the uncertainty of our data, and allows us to conclude that the same diffusion mechanism is responsible at both of these primary ion energies.

The measurement results can also be shown as the dependence of the total layer width, Δz, on temperature (see Fig. 5). This width becomes significantly narrower as the temperature is increased from 299 to around 400 K and does not seem to change until the temperature is greater than 703 K (where at 793 K the profiles broaden because of the increasing development of surface roughness).

3. Discussion

3.1. Room temperature RED data

Our observation of a linear dependence between the diffusion rates and the ion current density is a rather significant result, since this is precisely what would be expected from the theory developed by Dienes and Damask (G. J. Dienes and A. C. Damask, 1958) for RED. In the framework of their theory, this result is a consequence of the assumption that defect recombination (e.g. vacancyinterstitial recombination) is not the rate determining mechanism. Thus the linear relationship of D vs S_{Ag} shown in Fig. 3 demonstrates that our evaluation procedure can correctly describe the RED process.

The diffusion rate of grain boundary diffusion of Ag in Ni, extrapolated from high temperature data (A. B. Vladimirov, 1978) is approximately $D_b = 3.3 \times 10^{-19}$ cm^2/s at 300 K, a value considerably smaller than what is obtained here for the RED rate. The authors are not aware of other RED rate measurement carried out on the Ag/Ni system, except for the RIS measurement cited above (J. Fine et al., 1983). The diffusion rate was not evaluated in that study but can be estimated from the segregation rate constants that were obtained. Such an estimate yields $D_1 = 4.7 \times 10^{-17}$ cm^2/s and $D_4 = 1.9 \times 10^{-16}$ cm^2/s for 1 keV and 4 keV ion bombardment, respectively (the sputtering rates were $S_1 = 7 \times 10^{-3}$ nm/s and $S_4 = 3.1 \times 10^{-2}$ nm/s). These D values obtained in a completely different type type of measurement from what reported here, are in very good agreement with our D values shown in Fig.3.

Swartzfager et al. (D. G. Swartzfager et al., 1981) observed D values of the order of 10^{-16} cm^2/s in Cu-Ni, 10^{-17} cm^2/s in Au-Pd and 10^{-17} cm^2/s in Ag-Au alloys, using 2 keV Ne^+ sputtering at room temperature. Their sputtering rate, 5.2×10^{-3} nm/s, was comparable with some of our rates and the diffusion rates that we observe are surprisingly close to theirs (cf. Fig. 3). Li et al. (R. S. Li et al., 1985), however, obtained a diffusion rate around 1.1×10^{-14} cm^2/s for the Cu-Au system (2 keV Ar^+ bombardment) at room temperature. This high diffusion rate can be, at least in part, explained by the fact that the authors used a high current density (0.22 nm/s erosion rate), nearly 5 times the maximum rate used in the present study.

3.2. Temperature dependent RED

The negative Q values obtained in the present study are not consistent with thermal diffusion theory. The diffusion rate for thermal diffusion, D, can be expressed by

$$D = \gamma a^2 \nu_0 \exp\frac{S_m}{k} \exp\left(-\frac{E_F + E_m}{kT}\right) = D_0 \exp\left(-\frac{Q}{kT}\right) \qquad (8)$$

where γ is a geometrical coefficient, a is the lattice parameter (jump distance), ν_0 represents an effective frequency of vibration in the direction most favorable for jumping, S_m and E_m are the migration entropy and migration energy, kT is the Boltzmann factor, E_F is the energy of formation of the defects, and Q is the activation energy of the diffusion process. Since both E_F and E_m are positive quantities, then Q must be positive.

The theory of RED as described by Dienes and Damask (G. J. Dienes et al., 1958) also does not allow for $Q<0$. This theory is based on assumptions that the entire process is in a steady state and that point defects introduced by the radiation diffuse to sinks and annihilate. For these assumptions to be true, RED must be independent of temperature.

Furthermore, chemically driven demixing cannot lead to the separation of an interdiffusion region into two distinct layers (i.e. with one sharp interface) because, first, it would only lead to the formation of precipitates, and, second, at the low concentrations which occur in marker-layer systems the observed insignificant chemical effect on mixing (S.-J. Kim et al., 1988) strongly suggests that demixing would not be observable.

An analysis of our results could be performed on the basis of the generalized Fick's law:

$$J = D^* F \tag{9}$$

where D^* is the diffusivity (which may depend upon the concentrations of the components) and F is the driving force (the derivative of the chemical potential). This nonlinear equation is, at least in principle, capable of describing the entire phenomenon, including chemical forces and surface segregation. We will shortly discuss both phenomena in the context of our experiments.

For a vacancy mechanism of interdiffusion of real solute and solvent, Darken's result states (see e.g. P. G. Shewmon, 1963) that the diffusion rate of component, l, D_1, differs from its diffusion rate obtained in an ideal, or dilute solution, D_1^0, as

$$D_1 = D_1^0 \left(1 + \frac{d \ln \gamma_1}{d \ln N_1} \right) \tag{10}$$

where γ_1 is the activity coefficient and N_1 is the molar fraction of component 1. The second term in the parenthesis may be related to the heat of mixing. Cheng et al. (Y.-T. Cheng et al., 1984) applied this concept to cascade mixing and arrived at a formula

$$D^* = D(1 - 2\Delta H/RT) \tag{11}$$

where ΔH is the heat of mixing, R is the gas constant, and T is an effective temperature of 10^4 K (order of magnitude). This equation is valid for simple mixtures only, and for real mixtures additional terms appear in the parenthesis. For large positive heats of mixing, demixing could be expected on the basis

of this equation. This possibility was tested by Averback et al. (R. S. Averback et al., 1986), who found that there was less mixing in a Cu-Nb system at 295 K than at 6 K. This was interpreted as a sign of demixing by these authors, who claim that the Cu-Nb system is immiscible. However, according to Hansen (M. Hansen, 1958), the Cu-Nb system is probably simple eutectic and so the only experiment on demixing is, the least to say, inconclusive. On the other hand, metastable Ag-Ni alloys were obtained by cosputtering (M. Kitada, 1985 and L. Protin et al., 1986), laser surface alloying (C. W. Draper et al., 1980) and by ion-beam mixing (L. Buene et al., 1981).

Our time-dependent surface segregation experiments (cf. Fig. 1) show very clearly that diffusion occurs at room temperature. It can be assumed that if there is a chemical force that influences the diffusion, then it is proportional to the concentration gradient. The driving force in eq. (9) can then be expressed as

$$F = -\left(\frac{\partial c}{\partial z} \pm L\frac{\partial c}{\partial z}\right) \tag{12}$$

where L is a constant. The combination of (9) and (12) leads to a picture very similar to Darken's equation (10), but now the chemical force is introduced in the driving force, rather than into the diffusivity. It is clear that the sign of F will not change with the temperature unless L changes. Thus in a temperature region, where the mixing situation does not change substantially, F is of constant sign. If a system displays "normal" (concentration-gradient-driven) diffusion features at some temperature, then this will not change to uphill diffusion due to temperature changes. Thus, the mixing-demixing effect will not be qualitatively distinguishable from concentration-driven diffusion, although the magnitude of the experimental diffusion rate (mixing parameter) may be affected. In our Ag/Ni experiments, interface broadening due to RED (i.e. a process of mixing) was observed at room temperature; this process can not be reversed at elevated temperatures (i.e. demixing can not take place).

One possible mechanism which might affect the shape of the Ag peaks at elevated temperatures could be related to enhanced surface segregation at higher temperatures. Silver atoms situated between the Ag layer and the exposed Ni surface may be driven toward the surface by a combination of two forces: the concentration gradient from the Ag layer and the surface segregation of Ag, both of which are directed in this case toward the surface. Due to the higher sputtering rate of Ag, the segregation force will be constantly at work. When the sputtered surface passes the Ag layer, the concentration-gradient force's direction will be reversed (it will be directed into the specimen), but the segregation force will remain the same. The Ag peak could shift (U. Littmark et al., 1980) due to these phenomena toward the original specimen surface (toward earlier sputtering time). It is possible to check this concept

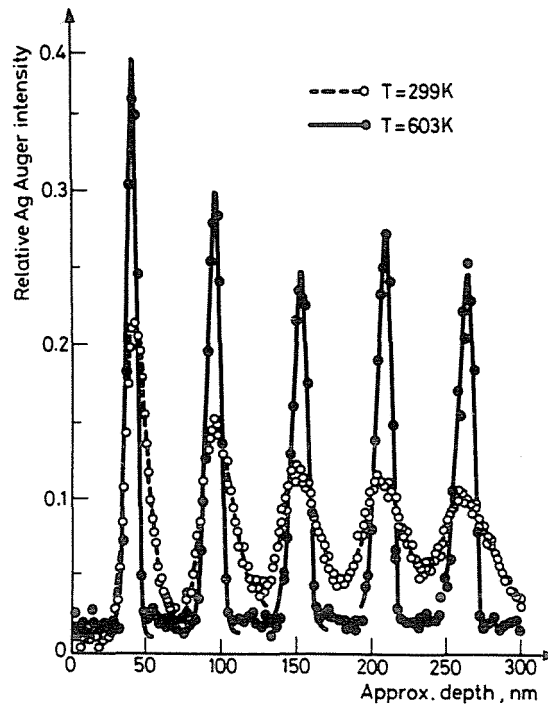

Fig. 6. Auger-electron depth profiles obtained at 299 K (data: ○; fit: dashed line), and 603 K (data: *; fit: solid line) superposed in order to show any possible effect of surface segregation. The time scale of one of the depth profiles was normalized in such a way that the starting times and the times for crossing the last (5th from the surface) Ag layer overlap. Any significant effect due to surface segregation at elevated temperature would shift the 1st Ag layer, as detected at this temperature, toward the surface

in the following way: two depth profiles, obtained at room temperature and at elevated temperature, are aligned so that the starting points (the original surface) and deepest (5th) Ag layer coincide (see Fig. 6). If the segregation is significantly more pronounced at higher temperatures than at room temperature then the leading edge of the Ag peaks obtained in the room temperature profile should appear at larger depths in this figure with the displacement of the first Ag layer being the largest. Obviously this is not the case and demonstrates that surface segregation does not play a dominant role in these measurements.

3.3. RED mechanism

In the previous sections, we have considered the driving forces responsible for the diffusion process. Now we turn to the defect mechanism which can allow for the diffusion observed. The very fact that RED takes place on

a time scale of minutes (both in experiments described here and by Fine et al., 1983), is reason enough to conclude that defect complexes, rather than simple point defects, are responsible for the diffusion observed. On the basis of the theory of radiation enhanced diffusion in solids (G. J. Dienes et al., 1958) we have estimated the number of the defects created by each bombarding particle, necessary to give rise to the observed diffusion rates, Y_d. The following values were obtained: $Y_{1d} = 1.9$ defects/ion (1 keV) and $Y_{4d} = 20.4$ defects/ion (4 keV) (D. Marton et al., 1988). These estimated Y_d values are based on the assumption that the Ag diffusion is related to the production of complex defects whose annealing time constants are long compared to that of the point defects; consequently point defects do not contribute to the observed diffusion rates. Although no experimental values exist for Y_d in Ag/Ni, results obtained by computer simulation techniques do exist for solids bombarded by keV ions and indicate that our values of Y_d are somewhat lower, but nevertheless close (D. S. Karpuzov et al., 1984, A. Vehanen et al., 1985).

Our experimental values for the range of radiation damage, which plays a role in RED (z_0), far exceed the mean values of the depth distribution of ballistic defects obtained in computer simulation calculations. These calculations also indicate the existence of a long exponential tail in the defect distribution (D. S. Karpuzov et al., 1984, A. Vehanen et al., 1985). Long-range radiation induced defects, lying in the tail of the defect distribution, have been experimentally detected using positron annihilation techniques in aluminium bombarded by low energy Ar^+ ions (A. Vehanen et al., 1985). It is also possible that the large z_0 values we observe result from the diffusion of defects initially created in the collision cascade itself; such diffusion can produce defect concentrations beyond that of the cascade and so can extend the range of radiation damage. This possibility also was pointed out by Ho (P. S. Ho, 1978).

The temperature dependence of the diffusion rate for radiation or bombardment induced RED can be explained in terms of processes involving complex defects. We therefore propose the following mechanism for RED: In solids, collisional processes result in the generation of point defects within the volume of the collision cascade itself. The lifetimes of these defects are not long enough to allow them to diffuse much beyond the collision cascade so they, consequently, cannot give rise to the extensive diffusion observed in RED. The shortlived point defects may, however, combine to form complex defects which may have rather long lifetimes and may themselves diffuse. Atom migration is made possible by encounters with these complex defects which extend far beyond the sputtered surface.

The concentration of these complex defects is temperature dependent; they may disintegrate into simple point defects which, because of their short lifetime, do not contribute significantly to diffusion. The steady-state concentration of complex defects, V, will depend on a quantity V_0, proportional to

the rate at which the complex defects are produced by irradiation, and on their binding energy, B:

$$V = V_0 \exp \frac{B}{kT} \tag{13}$$

From this relation, one may arrive at the following equation for the effective RED rate (D. Marton et al., 1988):

$$D = \gamma a^2 \nu_0 V_0 \exp \frac{S_m}{k} \exp\left(\frac{B - E_m}{kT}\right) = D_0 \exp\left(-\frac{Q}{kT}\right) \tag{14}$$

The right-hand side of this equation is similar in structure to that of eq. (12), but this equation has some new features which makes its interpretation quite different. First, the activation energy, Q, obtained here is not constrained to be positive and its sign will depend on the difference between the binding energy of the defect complex, involved in the RED process, and the energy of motion of the diffusant. These energies are both in the range of a few tenths of an eV, as various experiments and calculations show. For example, the binding energy of a divacancy in Ni is $B \simeq 0.5$ eV (W. Schule et al., 1982); the binding energy of a vacancy-Sb complex in Ni is $B = 0.5$ eV (M. H. Yoo, 1981); the migration energy of Ni self-interstitials is $E_m \simeq 0.6$—0.8 eV (W. Schule, 1982). It seems most likely that the type of defects responsible for RED are divacancies and solute-interstitial complexes. In a recent paper Hoff and Lam suggested that interstitial-Ge complexes contribute to RED in a Ni-Ge system (H. A. Hoff et al., 1988). Second, the absolute value of the activation energy in eq. (14) should be significantly smaller than the usual thermal diffusion activation energies, a fact which has so far been observed in all cases of ion-induced RED. Third, the preexponential factor, D_0, is linear with the production rate of the defects and accounts for the linear dependence of D on the sputtering rate, S.

Equation (14) is consistent with previous observations of ion-induced RED rates. Swartzfager et al. (D. G. Swartzfager et al., 1981) have reported data for Cu-Ni, Au-Pd and Ag-Au systems. The activation energies derived from their data are $Q = 0.025$, $Q = 0.055$ and $Q = 0.103$ eV, respectively. For the Cu-Ni other authors have reported differing results: Yabumoto et al. (M. Yabumoto et al., 1979) found less diffusion in this system at 200—300°C than at room temperature; they interpreted this result as being due to a decrease of the concentration of the excess defects caused by ion bombardment at elevated temperatures. Swartzfager et al. (D. G. Swartzfager et al., 1981) suggested, however, that what Yabumoto et al. observed was related to the lack of steady conditions in their measurement. More recently, however, Lam et al. (N. Q. Lam et al., 1985) published results which show no temperature

dependence for this system at temperatures below 400°C. Li and Koshikawa (R. S. Li et al., 1985) have reported $Q = 0.06$ eV for the Au-Cu system. Recently, Lam and Hoff (N. Q. Lam et al., 1988) reported data from which the value of $Q = 0.095$ eV can be derived for Si diffusion in Ni. As mentioned before, these energies are far smaller then the activation energies of thermal diffusion processes (e.g., $Q = 1.0$—2.2 eV for Au-Cu alloys, and $Q = 1.04$ eV for grain boundary diffusion of Ag in Ni (A. B. Vladimirov et al., 1978)).

Another manifestation of this annealing mechanism is the observed temperature dependence of the depth profiled layer width. The decrease of $\Delta z(299 \rightarrow 603$ K) can be ascribed to the large reduction in RED. This result is particularly significant because it suggests a possible way of improving depth resolution in sputter depth profiling, especially in systems where RED is significant and is temperature dependent.

4. Summary

Radiation enhanced diffusion measurements have been carried out by Auger sputter depth profiling of Ni/Ag multilayered thin-film structures in order to determine the effect of RED on interface broadening in sputter depth profile measurements. The interface broadening observed in this system is determined by a number of factors, the main two being surface roughening and RED. These two factors can be separated using the assumption that roughness leads to a symmetric profile shape, while an asymmetric shape is caused by RED. This concept is confirmed by our interface broadening results: the symmetric contribution (roughness) increases with depth (for subsequent Ag layers) while the asymmetric component (RED) remains independent of depth.

Effective diffusion rates, substantially higher than the grain boundary diffusivity of Ag in Ni at room temperature and proportional to the sputtering rates, were determined for primary ion energies of 1 keV and 4 keV. The values obtained are in good agreement with RIS rates determined in previous experiments. Defect complexes, rather than point defects, are likely to play an important role in RED. It is important to note that the range of the RED process (i.e. the range of the defects) is considerably greater than the range of ion mixing, and the time scale of the RED process is of the order of magnitude of minutes.

We have shown also that the RED of Ag in Ni induced by ion bombardment results in a diffusion rate which decreases with increasing temperature. This decrease in the RED rate cannot be explained simply on the basis of atom mobility. A model has been proposed in which long-lived complex defects can diffuse far beyond the range of the collision cascade.

These complex defects, however, may disintegrate at elevated temperatures, and so can result in a more limited migration of atoms. Observed temperature-dependent RED rates are accounted for by this model which suggests that it may be possible to control transport processes in RED through annealing. This possibility can have a significant impact on many collisionally initiated processes such as interface resolution in sputter depth profiling and defect generation and material transport in nuclear-power reactors.

Acknowledgements

Authors would like to thank B. Navinšek (J. Stefan Inst., Yugoslavia) who prepared the samples, and J. Manning (NIST), R. Kelly (IBM) and T. D. Andreadis (NRL) for helpful discussions.

References

ASHLEY, J. C., TUNG, C. J.: Surface & Interf. Anal., *4*, 52 (1982)
AVERBACK, R. S., PEAK, D., THOMPSON, L. J.: Appl. Phys., *A39*, 59 (1986)
BUENE, L., JACOBSON, D. C., NAKAHARA, S., POATE, J. M., DRAPER, C. W., HIRVONEN, J. K.: in Laser and Electron Beam Solid Interactions and Material Processing, Proc. of the Materials Res. Soc. Ann. Meeting, Boston, 1980, ed. J. F. Gibbons et al., North-Holland, 1981, p. 583
CHENG, Y.-T., VAN ROSSUM, M., NICOLET, M.-A., JOHNSON, W. L.: Appl. Phys. Lett., *45*, 185 (1984)
CHU, W. K., HOWARD, J. K., LAVER, L. F.: J. Appl. Phys., *47*, 4500 (1976)
COLLINS, R.: in Radiation Effects in Insulators 3, Proc. of the Third Internat. Conference, Guilford, 1985, ed. I. H. WILSON, R. P. WEBB, GORDON and BREACH, 1986, p. 167
DAVARYA, F., ROUSH, M. L., FINE, J., ANDREADIS, T. D., GOKTEPE, O. F.: J. Vac. Sci. Technol., *A1*, 467 (1983)
DIENES, G. J., DAMASK, A. C.: J. Appl. Phys., *29*, 1713 (1958)
DRAPER, C. W., PREECE, C. M., JACOBSON, D. C., BUENE, L. B., POATE, J. M.: in Laser and Electron Beam Processing of Materials, ed. C. W. White, P. S. Peercy, Acad. Press, 1980, p. 721
FARKAS, D., PASIANOT, R., TANGASWAMY, M., SAVINO, E. J.: Nucl. Instr. & Meth. in Phys. Res., *B16*, 183 (1986)
FINE, J., ANDREADIS, T. D., DAVARYA, F.: Nucl. Instr. & Methods, *209*, 521 (1983)
FINE, J., NAVINŠEK, B.: J. Vac. Sci. & Technol., *A3*, 1408 (1985)
HANSEN, M., ed.: Constitution of Binary alloys, 2nd ed. by K. Anderko, McGraw-Hill, New York, 1958
HART, R. R., DUNLAP, H. L., MARSH, O. J.: J. Appl. Phys., *46*, 1947 (1975)
HO, P. S.: Surface Sci., *72*, 253 (1978)
HOBBS, J. E., MARWICK, A. D.: Radiation Eff. Lett., *58*, 83 (1981)
HOBBS, J. E., MARWICK, A. D.: Nucl. Instr. & Meth. in Phys. Res., *B9*, 169 (1985)
HOFF, H. A., LAM, N. Q.: Surface Sci., *204*, 233 (1988)
KARPUZOV, D. S., ARMOUR, D. G.: J. Phys., *D17*, 853 (1984)
KIM, S.-J., NICOLET, M.-A., AVERBACK, R. S., PEAK, D.: Phys. Rev. *B37*, 38 (1988)

KITADA, M.: J. of Materials Sci., *20*, 269 (1985)
KORNBILT, L., ZAMORRODIAN, A. R., TOUGAARD, S., IGNATIEV, A.: Rad. Effects, *91*, 97 (1985)
LAM, N. Q., HOFF, H. A., WIEDERSICH, H., REHN, L. E.: Surface Sci., *149*, 517 (1985)
LAM, N. Q., HOFF, H. A.: Surface Sci., *193*, 353 (1988)
LI, R. S., KOSHIKAWA, T.: Surface Sci., 151, 459 (1985)
LITTMARK, U., HOFER, W. O.: Nucl. Instr. and Methods, *168*, 329 (1980)
MARTON, D., FINE, J.: Thin Solid Films, *151*, 433 (1987)
MARTON, D., FINE, J., CHAMBERS, G. P.: in Diffusion at Interfaces: Microscopic Concepts, ed M. GRUNZE, H. J. KREUZER and J. J. WEIMER (Springer-Verlag, Berlin, 1988), p. 111
MARTON, D., FINE, J., CHAMBERS, G. P.: Phys. Rev. Lett., *61*, 2697 (1988)
MARTON, D., FINE, J.: Thin Solid Films, in print Protin, L., Grenet, J., Fleury, G., Revue Phys. Appl., *21* (1986) 775
SCHULE, W.: in Point Defects and Defect Interactions in Metals, ed. J. Takamura, M. Doyama and M. Kiritani (Univ. Tokyo Press, Tokyo, 1982), p. 209
SCHULE, W., SCHOLZ, R.: in Point Defects and Defect Interactions in Metals, ed. J. Takamura, M. Doyama and M. Kiritani (Univ. Tokyo Press, Tokyo, 1982), p. 257
SHEWMON, P. G.: Diffusion in Solids, McGraw-Hill, New York, 1963
SWARTZFAGER, D. G., ZIEMECKI, S. B., KELLEY, M. J.: J. Vac. Sci. Technol., *19*, 185 (1981)
VANDERVORST, W., SHEPHERD, F. R., SWANSON, M. L., PLATTNER, H. H., WESCOTT, O. M., MITCHELL, I. V.: Nucl. Instr. & Meth. in Phys. Res., *B15*, 201 (1986)
VEHANEN, A., MAKINEN, J., HAUTOJARVI, P., HUOMO, H., LAHTINEN, J., NIEMINEN, R. M., VALKEALAHTI, S.: Phys. Rev., *B32*, 7561 (1985)
VLADIMIROV, A. B., KAYGORODOV, V. N., KLOTSMAN, S. M., TRAKHTENBERG, I. SH.: Fiz. Metal. Metalloved., *45*, 1015 (1978); (English transl.: Phys. Met. Metall., *45*, 100 (1979)
YABUMOTO, M., KAKIBAYASHI, H., MOHRI, M., WATANABE, K., YAMASHINA, T.: Thin Solid Films, *63*, 263 (1979)
YOO, M. H.: J. Phys. *F11*, L65 (1981)

D. MARTON, J. FINE
National Institute of Standards and Technology
Gaithersburg, MD 20899, USA